



Temperature of the inner-core boundary of the Earth: Melting of iron at high pressure from first-principles coexistence simulations

Dario Alfè*

Department of Earth Sciences and Department of Physics and Astronomy, Materials Simulation Laboratory, and London Centre for Nanotechnology, UCL, Gower Street, London WC1E 6BT, United Kingdom

(Received 11 December 2008; published 11 February 2009)

The Earth's core consists of a solid ball with a radius of 1221 Km, surrounded by a liquid shell which extends up to 3480 km from the center of the planet, roughly half way toward the surface (the mean radius of the Earth is 6373 km). The main constituent of the core is iron, and therefore the melting temperature of iron at the pressure encountered at the boundary between the solid and the liquid [the inner-core boundary (ICB)] provides an estimate of the temperature of the core. Here I report the melting temperature of Fe at pressures near that of the ICB, obtained with first-principles techniques based on density-functional theory. The calculations have been performed by directly simulating solid and liquid iron in coexistence and show that and at a pressure of ~ 328 GPa iron melts at $\sim 6370 \pm 100$ K. These findings are in good agreement with earlier simulations, which used exactly the same quantum-mechanics techniques but obtained melting properties from the calculation of the free energies of solid and liquid Fe.

DOI: [10.1103/PhysRevB.79.060101](https://doi.org/10.1103/PhysRevB.79.060101)

PACS number(s): 64.70.D-, 71.15.Pd, 91.45.Kn

The study of iron under extreme conditions has a long history. In particular, numerous attempts have been made to obtain its high-pressure melting properties.¹⁻⁹ Experimentally, Earth's core conditions can only be reproduced by shock wave (SW) experiments in which a high-speed projectile is fired at an iron sample, and upon impact high-pressure and high-temperature conditions are produced. By varying the speed of the projectile it is possible to investigate a characteristic pressure-volume relation known as the Hugoniot¹⁰ and even infer temperatures, although a word of caution here is in order as temperature estimates are often based on the knowledge of quantities such as the constant volume specific heat and the Grüneisen parameter, which are only approximately known at the relevant conditions.⁷ If the speed of the projectile is high enough, the conditions of pressure and temperature are such that the sample melts, and it is therefore possible to obtain points on the melting curve, of course with the caveat mentioned above about temperature measurements. An alternative route to high-pressure, high-temperature properties is the use of diamond anvil cells (DAC) in which the sample is surrounded by a pressure medium and statically compressed between two diamond anvils. In DAC experiments pressure and temperatures can be directly measured, and therefore these techniques should in principle be more reliable to investigate melting properties. Unfortunately, in the case of iron it is not so and there is a fairly large range of results obtained by different groups.¹⁻⁶

An alternative approach used for the past ten years or so has been to employ theory—and in particular quantum-mechanics techniques based on density-functional theory (DFT)—to calculate the high-pressure melting curve of iron. A number of groups have used different approaches to the problem. Our own strategy has been to calculate the Gibbs free energy of solid and liquid iron and then obtain the melting curve by imposing their equality for any fixed pressure. We obtained a melting temperature of ~ 6350 K at 330 GPa.¹¹ The approach of Belonoshko *et al.*¹² was to fit an embedded atom model (EAM) to first-principles calculations

and then calculate the melting curve of the EAM. They obtained a temperature of ~ 7050 K at 330 GPa. The approach of Laio *et al.*¹³ was similar, although they refitted their optimized potential model (OPM) to first-principles calculations in a self-consistent way. They obtained a melting temperature of ~ 5400 K at 330 GPa. We later reconciled the results of Belonoshko *et al.*¹² with ours by showing that the difference was due to a difference in free energies between their EAM and our DFT.¹⁴ A similar argument would be responsible for the difference between our results and those of Laio *et al.*¹³

Here I am using an approach to melting which is independent of the free-energy technique used earlier,^{11,15,16} and the main motivation of this work is to provide an alternative route to the calculation of the melting properties of Fe. The method employed here is that of the coexistence of phases in which solid and liquid iron are simulated in coexistence. The first time that the method was used in the context of first-principles calculations was for the low-pressure melting curve of aluminum,¹⁷ where it was shown to deliver the same results as the free-energy method.¹⁸ It was later applied to compute the melting curve of LiH,¹⁹ hydrogen,²⁰ and MgO.²¹

The coexistence method is intrinsically expensive as it requires large simulation cells and long simulations. It can be applied in a number of different ways. Here I have used the *NVE* ensemble, i.e., constant number of atoms N , constant volume V , and constant internal energy E . In the *NVE* ensemble, for each chosen volume V there is a whole range of energies E for which solid and liquid can coexist for a long time; the average temperature and pressure along the simulation then provide a point on the melting curve. If the energy E is above (below) the range where coexistence can be maintained, the system will completely melt (solidify), and the simulation does not provide useful melting properties information. It should be pointed out that any finite system will eventually melt or solidify if simulated for long enough due to spontaneous fluctuations. However, melting (solidifi-

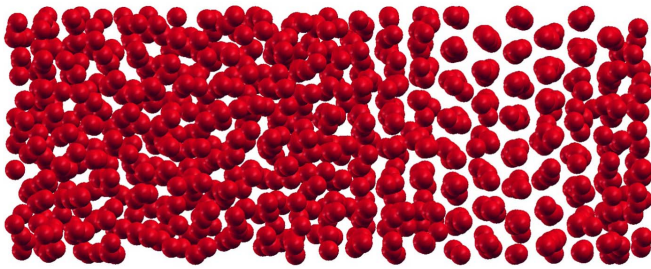


FIG. 1. (Color online) Snapshot of a DFT molecular-dynamics simulation showing solid and liquid iron in coexistence. The simulation cell contains 980 atoms.

cation) resulting from a too-high (low) value of E typically appears on much shorter time scales.

The present calculations have been performed with density-functional theory with the generalized gradient approximation known as PW91 (Ref. 22) and the projector augmented wave method^{23,24} as implemented in the VASP code.²⁵ An efficient extrapolation of the charge density was employed.²⁶ Single-particle orbitals were expanded in plane waves with a cutoff of 300 eV, and I used the finite temperature implementation of DFT as developed by Mermin.²⁷ These settings are exactly equivalent to those used in our previous work,^{11,15,16} so the melting properties obtained here will be directly comparable to those early ones. The simulations have been performed on hexagonal closed packed (hcp) cells containing 980 atoms ($7 \times 7 \times 10$), using the Γ point only. For the temperatures of interest here the use of the Γ point provides completely converged results. The time step in the molecular-dynamics simulations was 1 fs, and the self-consistency on the total energy was 2×10^{-5} eV. With these prescriptions the drift in the constant of motion was ~ 0.5 K/ps.

The coexistence simulations were prepared by starting from a perfect hcp crystal, which was initially thermalized to ~ 6300 K for 1 ps. Then half of the atoms in the cell were clamped and the temperature was raised to a very high value to melt the other half of the cell. Once good melt was obtained, the temperature was reduced back to 6300 K and the system thermalized for one additional ps, after which the simulation was stopped, new initial velocities were assigned to the atoms, and the simulation continued in the microcanonical ensemble. The simulations were monitored using the density profile, calculated by dividing the simulation cell in 100 slices parallel to the solid-liquid interface and counting the number of atoms in each slice; in the solid region this is a periodic function, with large number of atoms if the slice coincides with an atomic plane, and small values if it falls between atomic layers. In the liquid region it fluctuates randomly around some average value.

I performed five different simulations, starting with different amounts of internal energies E provided to the system by assigning different initial velocities to the atoms. The simulation with the highest value of E completely melted after ~ 6 ps. The one with the lowest amount of E solidified after ~ 11 ps. Among the other three, one melted after ~ 14 ps, one after ~ 24 ps, while the last one has remained in coexistence for the whole length of ~ 25 ps. However, most of

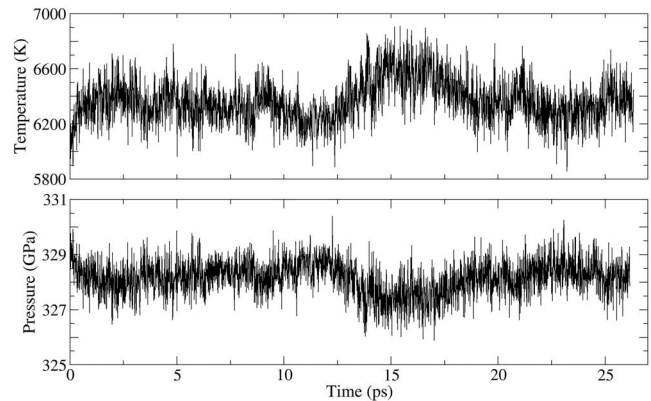


FIG. 2. Temperature (upper panel) and pressure (lower panel) for a simulation of solid and liquid iron in coexistence.

these simulations were coexisting for long enough so that useful melting information from the period of coexistence could actually be extracted in almost all cases. A snapshot of a simulation with solid and liquid in coexistence is shown in Fig. 1.²⁸

In Fig. 2 I display the temperatures and the pressures corresponding to the simulation that remained in coexistence for the whole 25 ps length, which provides a melting point $(p, T) = (328 \pm 1 \text{ GPa}, 6370 \pm 100 \text{ K})$. It is interesting to notice a temperature excursion in the simulation after ~ 15 ps, which lasts for ~ 5 ps. This temperature variation is anticorrelated with a pressure variation and corresponds to a temporary loss of some liquid in the cell, with latent heat of fusion converted into kinetic energy and volume of fusion responsible for the drop in pressure. Large excursions of these type may provoke *accidental* melting (or freezing) even if the internal energy E is within the range of coexistence. This problem is mitigated by the use of large simulation cells, and therefore this is one of the reasons why large simulation cells are needed in conjunction with the coexistence approach.

In Fig. 3 I show a simulation that eventually solidified; however, as mentioned above, coexistence was maintained

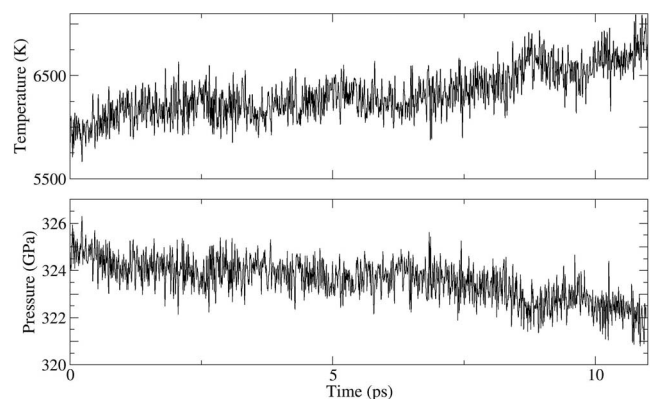


FIG. 3. Temperature (upper panel) and pressure (lower panel) for a simulation of solid and liquid iron in coexistence. The system eventually completely solidifies, with a drop in pressure and an increase in temperature due to release of volume and latent heat of fusion, respectively.

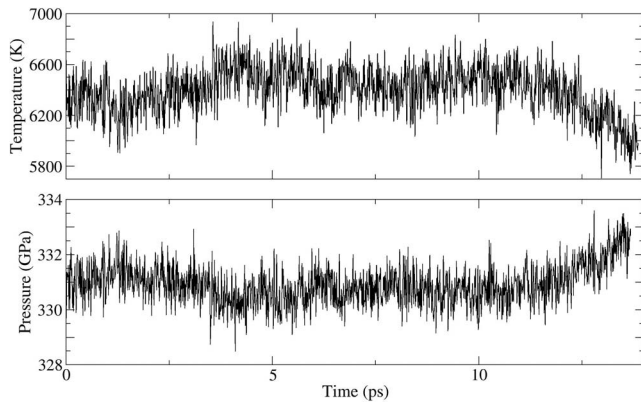


FIG. 4. As in Fig. 3, but here the system eventually melts.

for a long period, and the information gathered by the central part of the simulation can still be used to obtain a point on the melting curve, and the result is $(p, T) = (324 \pm 1 \text{ GPa}, 6250 \pm 100 \text{ K})$, which is consistent with the previous point. Similarly, in Fig. 4 I show one of the simulations that eventually melted, and by taking the average temperature and pressure from the central part of the simulation I get $(p, T) = (331 \pm 1 \text{ GPa}, 6430 \pm 100 \text{ K})$, which is also consistent with the other previous two points.

The c/a value used in the simulations was fixed at 1.6, which resulted in slightly nonhydrostatic conditions. To study the effect of nonhydrostaticity, and that of the relatively small size of the simulation cells, I have performed simulations using a classical EAM, adapted to deliver results very close to the present *ab initio* techniques.¹⁴ I have performed simulations on cells containing 7840 atoms ($14 \times 14 \times 20$) and found that at a pressure of 324 GPa the effect of using a small cell containing only 980 atoms is to raise the melting temperature by $\sim 100 \text{ K}$. The *ab initio* nonhydrostatic conditions with $c/a=1.6$ are similarly reproduced by the EAM, which also shows that with $c/a=1.65$ the simulations are almost exactly under hydrostatic conditions.²⁹ The effect of the nonhydrostaticity with $c/a=1.6$ is to reduce the melting temperature by $\sim 100 \text{ K}$ so that the combined effects of nonhydrostaticity and small size cancel each other. A final check was performed by repeating the simulations using 62 720 atom cells ($28 \times 28 \times 40$), which showed essentially no differences with the results obtained using 7840 atom cells.

All the present first-principles coexistence results are displayed in Fig. 5, which also contains experimental and previous theoretical results. The filled square corresponds to the simulation which maintained coexistence throughout (Fig. 2), while the empty squares to the other four simulations for which the final part has been discarded. As noted above, it is clear that all simulations provide similar melting points, with the exception perhaps of the point corresponding to the simulation that melted only after $\sim 6 \text{ ps}$ (point at highest temperature in Fig. 5). The comparison of the present results with the earlier melting curve obtained using the free-energy approach¹¹ shows excellent agreement, and the two sets of data therefore support each other. I also report on the same figure the DAC experiments of Refs. 1–4 and 6, the SW experiments of Refs. 7–9, and the calculations of Refs. 12

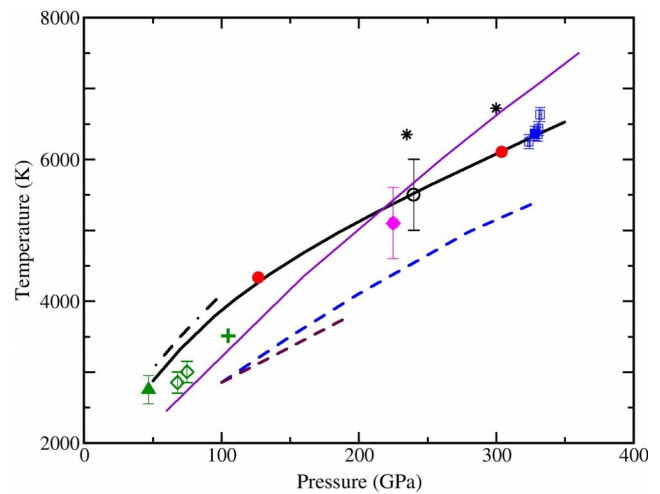


FIG. 5. (Color online) Comparison of melting curve of Fe from present calculations with previous experimental and *ab initio* results. Blue filled square: DFT coexisting simulation for over 25 ps; blue open squares: DFT coexisting simulations ending up to complete solids or liquids and results are gathered from the region of coexistence; black heavy solid curve: DFT melting curve from Ref. 11; long-dashed blue curve: DFT-OPM results of Ref. 13; light purple solid curve: DFT-EAM results of Ref. 12; filled red circles: DFT-EAM “corrected” results (see text); black chained and maroon dashed curves: DAC measurements of Refs. 1 and 2; green open diamonds: DAC measurements of Ref. 3; green plus: DAC measurement of Ref. 6; green filled triangle: DAC measurement of Ref. 4; and black stars, black open circle and pink filled diamond: shock experiments of Refs. 7–9. Error bars are those quoted in original references.

and 13. As mentioned above, we identified the reasons of the differences between our melting curve and that calculated by Belonoshko *et al.*¹² being the free-energy differences between their EAM and our DFT. Once these differences are taken into account it is possible to “correct” the EAM melting curve. The two red dots on the figure show the corrected EAM results at two different pressures, which agree with our DFT melting curve.

In conclusion, I have presented here calculations for the melting temperature of iron under Earth’s core conditions, obtained with density-functional theory and the technique of the coexistence of phases. The DFT techniques are the same as those employed in our earlier calculations, where we computed the melting curve using the free-energy approach.^{11,15,16} The consistency between the present calculations and those early ones is expected because the DFT technicalities are the same and provide an independent check on the accuracy of those early free-energy calculations. The DFT melting temperature of Fe at a pressure of $\sim 330 \text{ GPa}$ is therefore confirmed to be in the region of $\sim 6300\text{--}6400 \text{ K}$.

The next question that one might ask is: how accurate is DFT for this problem? We argued in our previous work that DFT should indeed be quite reliable mainly because solid and liquid iron have very similar structures so that possible errors would largely cancel between the two phases. How-

ever, we also pointed out that DFT does not seem to reproduce the zero-temperature pressure-volume equation of state of hcp iron completely correctly, possibly underestimating the pressure by $\sim 2.5\%$. We then argued that this error could propagate to the melting curve, resulting in a lowering of temperatures which at a pressure of 330 GPa could be in the region of ~ 150 K.¹¹ This would bring the melting temperature of Fe at ICB condition to ~ 6200 K. It will be interesting to revisit this problem with more accurate quantum-mechanics techniques, and we are planning to do so by using quantum Monte Carlo. We will report on these results in due course.

This work was conducted as part of a EURYI scheme award as provided by EPSRC-GB (see www.esf.org/euryi). Calculations have been performed on the U.K. national facility HECToR using allocation of time from the Mineral Consortium and from a EPSRC-GB Capability Challenge grant. Calculations were also performed on the UCL research-computing facility Legion and initially on the Cambridge High Performance facility Darwin. Simulations were typically run on 256 cores, each molecular-dynamics step of 1 fs taking ~ 7.5 min.

*d.alfè@ucl.ac.uk

- ¹Q. Williams, R. Jeanloz, J. D. Bass, B. Svendsen, and T. J. Ahrens, *Science* **236**, 181 (1987).
- ²R. Boehler, *Nature (London)* **363**, 534 (1993).
- ³G. Shen, H. Mao, R. J. Hemley, T. S. Duffy, and M. L. Rivers, *Geophys. Res. Lett.* **25**, 373 (1998).
- ⁴A. P. Jephcoat and S. P. Besedin, *Philos. Trans. R. Soc. London* **354**, 1333 (1996).
- ⁵S. K. Saxena, G. Shen, and P. Lazor, *Science* **264**, 405 (1994).
- ⁶Y. Ma, M. Somayazulu, G. Shen, H. K. Mao, J. Shu, and R. J. Hemley, *Phys. Earth Planet. Inter.* **143–144**, 455 (2004).
- ⁷J. M. Brown and R. G. McQueen, *J. Geophys. Res.* **91**, 7485 (1986).
- ⁸J. H. Nguyen and N. C. Holmes, *Nature (London)* **427**, 339 (2004).
- ⁹C. S. Yoo, N. C. Holmes, M. Ross, D. J. Webb, and C. Pike, *Phys. Rev. Lett.* **70**, 3931 (1993).
- ¹⁰J.-P. Poirier, *Introduction to the Physics of the Earth's Interior* (Cambridge University Press, Cambridge, 1991).
- ¹¹D. Alfè, G. D. Price, and M. J. Gillan, *Phys. Rev. B* **65**, 165118 (2002).
- ¹²A. B. Belonoshko, R. Ahuja, and B. Johansson, *Phys. Rev. Lett.* **84**, 3638 (2000).
- ¹³A. Laio, S. Bernard, G. L. Chiarotti, S. Scandolo, and E. Tosatti, *Science* **287**, 1027 (2000).
- ¹⁴D. Alfè, G. D. Price, and M. J. Gillan, *J. Chem. Phys.* **116**, 7127 (2002).
- ¹⁵D. Alfè, M. J. Gillan, and G. D. Price, *Nature (London)* **401**, 462 (1999).
- ¹⁶D. Alfè, G. D. Price, and M. J. Gillan, *Phys. Rev. B* **64**, 045123 (2001).
- ¹⁷D. Alfè, *Phys. Rev. B* **68**, 064423 (2003).
- ¹⁸L. Vočadlo and D. Alfè, *Phys. Rev. B* **65**, 214105 (2002).
- ¹⁹T. Ogitsu, E. Schwegler, F. Gygi, and G. Galli, *Phys. Rev. Lett.* **91**, 175502 (2003).
- ²⁰S. A. Bonev, F. Schwegler, T. Ogitsu, and G. Galli, *Nature (London)* **431**, 669 (2004).
- ²¹D. Alfè, *Phys. Rev. Lett.* **94**, 235701 (2005).
- ²²Y. Wang and J. P. Perdew, *Phys. Rev. B* **44**, 13298 (1991); J. P. Perdew, J. A. Chevary, S. H. Vosko, K. A. Jackson, M. R. Pederson, D. J. Singh, and C. Fiolhais, *ibid.* **46**, 6671 (1992).
- ²³P. E. Blöchl, *Phys. Rev. B* **50**, 17953 (1994).
- ²⁴G. Kresse and D. Joubert, *Phys. Rev. B* **59**, 1758 (1999).
- ²⁵G. Kresse and J. Furthmüller, *Phys. Rev. B* **54**, 11169 (1996).
- ²⁶D. Alfè, *Comput. Phys. Commun.* **118**, 31 (1999).
- ²⁷N. D. Mermin, *Phys. Rev.* **137**, A1441 (1965).
- ²⁸Figure realized with the XCRYSDENS software: A. Kokalj, *Comp. Mater. Sci.* **28**, 155 (2003) (code available from <http://www.xcrysden.org/>).
- ²⁹Simulations were also performed in the NpH ensemble (constant pressure p and enthalpy H) using the algorithm developed by E. R. Hernandez, *J. Chem. Phys.* **115**, 10282 (2001).